Effect of Calcium Expansive Additives on the Performance of Granite-Based Geopolymers for Zonal Isolation in Oil and Gas Wells

Foster Dodzi Gomado[1]*, Mahmoud Khalifeh[1], Arild Saasen[1], Susana G. Sanfelix[2], Anna-Lena Kjøniksen[2], and Jan Aage Aasen[1]

[1]Department of Energy and Petroleum Engineering, Faculty of Science and Technology, University of Stavanger
[2]Department of Engineering, Faculty of Computer Science, Engineering and Economics, Østfold University College

Summary

Geopolymers have emerged as a promising alternative to Portland cement for oil and gas wells. Achieving effective zonal isolation by use of geopolymers may require controlling their expansion. This study investigates the effect of calcium oxide (CaO) as an expansive agent on the performance of geopolymer-based sealing materials. Specifically, we explore the impact of CaO reactivity on various material properties using isothermal calorimetry, Brunauer-Emmett-Teller (BET) surface area analysis, linear expansion (LE) test, shear bond strength, compressive strength, and hydraulic bond strength (HBS). Our results indicate that CaO reactivity is a critical factor affecting the properties and performance of geopolymers for zonal isolation. Lower reactivities are associated with longer induction periods and lower heat evolution, which in turn increase LE. While lower reactivity decreases compressive strength, it increases shear bond strength. However, the CaO with the lowest reactivity resulted in a very low HBS due to matrix cracking and leakage. Therefore, optimizing the reactivity of CaO expansive agents is essential to enhancing the properties of geopolymer-based sealing materials for oil and gas wells. Shown in this paper is the successful application of CaO as an expansive agent for granite-based geopolymers at shallow depths in oil and gas wells.

Introduction

Oil and gas production is highly dependent on maintaining the integrity of the well throughout the entire production cycle. Similarly, the efficiency of geothermal and CO_2 injection wells also relies on the well performance. Well integrity is defined by NORSOK D-010 as "the application of the technical, operational, and organizational solution to reduce the risk of uncontrolled release of formation fluids through the life cycle of a well" (*NORSOK Standard D-010* 2021). The combination of cementing and other drilling and completion operations is deployed to minimize the risk of the uncontrolled release of formation fluids. The purpose of cement in a well is to prevent liquid and gas flow through the annuli and other escape paths. Effective cementing should therefore be prioritized for enhanced reliability and safety in oil and gas production. For cement to achieve this purpose, it needs to be impermeable enough to achieve both hydraulic and mechanical isolation. In addition, the cement must bond well with the casing and the formation, as well as possess sufficient mechanical strength. In-depth data analysis (Aslani et al. 2022; Davies et al. 2014; Gomado et al. 2022; Ogienagbon and Khalifeh 2022; Liu et al. 2023; Vignes 2011; Zheng et al. 2022) shows a high probability of the cement failing as a result of the dynamic downhole conditions in terms of pressure, temperature, and chemical reactions, which might cause physiochemical changes in the cement, thus deteriorating the well integrity in most wells. These failures result in a reduction of the strength and the cement bonding to the casing or the formation.

Portland cement is commonly used for zonal isolation purposes in wells due to its availability and competitive price. However, CO_2 emissions related to the production of conventional cement have become a significant concern, as well as other limitations such as durability and chemical attacks (Khalifeh 2016; Olvera et al. 2019; Panchmatia et al. 2020; Vrålstad et al. 2016). Therefore, geopolymers have emerged as an alternative for zonal isolation operations. Geopolymers are inorganic polymers usually formed from alkali activation of aluminosilicates (Chamssine et al. 2021; Davidovits 1994, 2002). The commonly used precursors are metakaolin, kaolin, rice husk, fly ash, and blast furnace slag (Nahm et al. 1994). Several studies have explored the use of geopolymers for oil and gas well applications (Adjei et al. 2022; Chamssine et al. 2021; Chen et al. 2020; Gomado et al. 2023; Khalifeh et al. 2017; Khalili et al. 2022; Kimanzi et al. 2020; Omran et al. 2022). Geopolymers are considered a promising candidate for oil and gas applications due to excellent mechanical properties, enhanced resistance to acid attacks, and much lower greenhouse gas emissions than Portland cement (Davidovits 2013; McLellan et al. 2011; Mehta and Siddique 2017; Salehi et al. 2017; Sambucci et al. 2021). Geopolymers also undergo less chemical shrinkage than conventional Portland cement (Olvera et al. 2019; Panchmatia et al. 2020). Because geopolymers are affected by the activator type, mineral admixtures deployed in the formulation, chemical additives, and curing conditions (Zhang et al. 2022a), it is important to develop an optimal recipe for the considered application. Also, geopolymers show strong bond with the coating of the steel casing (Moreira et al. 2023).

To ensure effective bonding of cement, there should be good contact between the cement and the casing or surface to minimize contaminations. Some techniques to ensure effective bonding are treating the casing or pipe surfaces, using shrinkage-reducing agents (i.e., expansive agents) to mitigate shrinkage, and increasing the chemical bonding activity of the cement using treatment chemicals (Root and Calvert 1971). Moreover, the well temperature and pressure should be estimated. For this purpose, the deployment of expansive agents as

*Corresponding author; email: foster.d.gomado@uis.no

Original SPE manuscript received for review 24 March 2023. Revised manuscript received for review 7 July 2023. Paper (SPE 217431) peer approved 10 July 2023.

a means of ensuring effective bonding will be the focus. In oil and gas operations, expansive agents (salts) and fillers are commonly used for improving cement bonding to the casing or the formation. These additives work either by maintaining the volume of the slurry upon setting (in the case of a filler) or by increasing the volume of the slurry upon setting (through the formation and growth of crystals). Shrinkage-reducing agents include fillers, expansive salts, polymers, and nanoparticles (Aslani et al. 2022; Jafariesfad et al. 2017; Zhang et al. 2022b). A stable matrix is required to prevent the flow of fluids through the bulk cement. In addition, optimal expansion levels are required to build stress at the interface at rock/casing to improve the bonding. The use of expansive agents will therefore be of prime interest in this research, with a focus on CaO as the expanding agent.

Achieving optimal expansion without compromising the mechanical properties is highly dependent on the reactivity of the expansive agent (hydration rate of the salts). The hydration of CaO is related to factors such as the geochemistry of the source rocks used in the production of CaO and the calcination temperature. These two factors play a role in the microstructure and specific surface areas, thus affecting the hydration rate (Vola et al. 2019). High calcination temperature tended to reduce the specific area, thus affecting the hydration rate. Expansive salts that hydrate quickly (e.g., CaO and MgO) have been found to give rise to less expansion (Appah and Reichetseder 2001; Ghofrani and Plack 1993). Ghofrani and Plack (1993) observed that the high reactivity of the expansive salts leads to quick hydration. Accordingly, most of the agent is consumed during the cement hydration process rather than facilitating the crystal growth process, resulting in little or no changes in the volume of the hardened cement. Expansion effects are usually optimized when the hydration of the expansive agent takes place during the gelation and early hardening phases of the cement. Late hydration of the expansive salts during the hardening stage of the cement (in the case of extremely low reactive salts) could be detrimental as the hydration products and the growth of the crystals can generate high internal stresses, which might fracture the matrix of the cement. This indicates that there should be an optimization between the expansion salts and the hydration processes of the cementitious materials.

Different shrinkage-reducing admixtures have been studied in geopolymer systems for oil and gas applications. Panchmatia et al. (2020) tested zinc-based and aluminum-based expansive additives on fly-ash-based geopolymers at elevated temperatures and pressures, achieving a shrinkage reduction of 35%. Humairah et al. (2020) also tested the viability of MgO and an elastomer in a geopolymer system. They revealed that both additives increase early expansion development but that MgO mostly supports early expansion rather than overall expansion. However, the reactivities of these expansive agents were not examined in these studies. In addition, the impact of CaO expansive additives on the performance of geopolymers has been hardly explored compared to its Portland cement counterpart. To facilitate the mass adoption of geopolymers in oil and gas applications, an in-depth understanding of how CaO expansive additives affect the performance of geopolymers in terms of their bonding capabilities is necessary. In a wellbore, there are two criteria to ensure effective bonding, namely shear bond and hydraulic bond (Nelson and Guillot 2006), as the matrix permeability of cementitious materials have been reduced to a satisfactory level. The shear bond estimates the cement plug's ability to mechanically support itself and stay in position, whereas HBS is the ability to inhibit flow at the interface. In addition to the above, the compressive strength of the material should be enough to maintain its mechanical integrity at downhole stresses.

This paper examines the impact of CaO additives and their reactivities on the performance of granite-based geopolymers in terms of solid-state properties such as LE, compressive strength, shear bond strength, and HBS. Also, this study explores the effect of heat treatment on the hydration rates of CaO as a means of optimizing the expansion of the CaO in granite-based geopolymers.

Experimental Procedures

To evaluate the impact of different CaO reactivities on the geopolymer systems, CaO was heat-treated, characterized, and tested as a geopolymer additive.

Preparation of CaO. A commercial CaO was heat-treated in an oven at temperatures of 900°C, 1200°C, and 1400°C. The selected heat treatment temperature was based on the temperature required to break down carbonates and other impurities in the CaO as well as to achieve enough sintering effect to reduce the hydration rate of the CaO for the study. One hundred grams of CaO was weighed into an alumina crucible and placed in the oven. The oven was set to ramp up to the targeted temperature in 1 hour and 30 minutes. The temperature was then held at the targeted temperature for 3 hours, after which the samples were left to cool down. A stone-like sample was formed at 1200°C and 1400°C. These samples were therefore broken down into smaller pieces and milled in a disc miller at 700 rev/min for 5 minutes for fineness. CaO particles treated at 900°C, 1200°C, and 1400°C are denoted HT-900, HT-1200, and HT-1400, respectively.

BET Surface Area. A TriStar II 3020 device was used to determine the BET surface area of CaO treated at different temperatures. The BET device works on the adsorption of nitrogen gas on the surfaces of the various CaO. The procedure for the test is as follows:

- One gram of the sample was weighed into the sample holders and then connected to a vacuum and degassed at 200°C for 2 hours.
- The samples were then attached to the Tristar II 3020 device, and the N_2 gas adsorption test was conducted, which was then used to estimate the BET surface area from its software program.

Reactivity of CaO. The ASTM D4644-16 standard (*ASTM D4644-16* 2016) describes a reactivity test for quick lime in water. According to this standard, reactivity is divided into three categories based on the time (t_{60}) required to increase a mixture of water and CaO to a temperature of 60°C in an isothermal environment. The classification is high reactivity ($t_{60} < 3$ minutes), medium reactivity (3 minutes < $t_{60} < 6$ minutes) and low reactivity ($t_{60} > 6$ minutes). However, because high amounts of CaO are required for this standardized test, an isothermal calorimeter was used to measure the heat evolution behavior of the CaO with time, which correlates with the hydration rates of the different CaO used in this study. Isothermal calorimetry was performed in an eight-channel thermal activity monitor instrument using admix glass ampoules.

- Pastes were prepared in situ by using admix ampoules to obtain the very early heat flow directly after the addition of water to the CaO. An amount of CaO equal to 0.51 g was weighted into the glass ampoule, and 3.0 g of water was introduced in the syringes (corresponding to the total mass of water in the slurry design).
- The prepared admix ampoules were introduced into the calorimeter to be thermally equilibrated. Once equilibrated, the recording of the heat flow was started, followed by emptying the water from the syringes into the glass ampoules. The samples were manually stirred for 1 minute using a small stirrer inside the ampoules. The heat flow was monitored for up to 2 days at 25°C.

As the development of expansive agents for geopolymers is a new research frontier, there are currently no specific standards in terms of values for their specific properties. Therefore, the existing testing procedures for cement are being applied to investigate the

performance and reactivity of these expansive agents in geopolymers. In addition, isocalorimetry is used to determine the reactivity of the expansive agents, which represents a novel approach compared to the standards set by ASTM for evaluating CaO.

Particle Size Distribution. The particle size distribution of the CaO particles was done using a laser diffraction Metasizer 3000. For this test, 6 g of the sample was weighed in the sample holders. The test commenced with putting in the density of the sample, which is 3.34 g/cm^3. The experiment is initiated in the software module until there is no sample holder.

Slurry Preparation and Geopolymer Composition. In this study, two different mixers were used to prepare the slurries for various tests. A high-speed API mixer was used for the LE test, the shear bond strength test, and the compressive test, which requires approximately 600 mL. Meanwhile a Hobart N50-60 commercial blender was used for the hydraulic sealability test due to its ability to handle larger quantities than the API blender (3.2 L of slurry was required for the hydraulic sealability test). It is important to note that the mixing energy difference between these mixers was not the focus of this work.

Small Slurry Volume Preparation.

- The geopolymers were prepared by weighing all the solid precursors with/without 1.1 wt% of the heat-treated CaO into a bowl, which was shaken manually for 1 minute to ensure an even mixture.
- Afterward, the solid phase was introduced into the liquid phase (4 M KOH in water).
- When using the API mixer, the solid phase was introduced into the liquid during the first 15 seconds at 4,000 rev/min, followed by an extra 35 seconds at 12,000 rev/min (API RP 10B-2 2019).

Large Slurry Volume Preparation.

- For the large-volume slurry, the solid precursors were introduced into the liquid phase during the first 5 minutes, using Speed Level 1 of the Hobart mixer.
- Afterward, stirring was conducted at Speed Level 2 for an additional 25 minutes.

The detailed composition of the materials for the geopolymers are listed in **Table 1.**

Component of the Geopolymer Cement	Description	Total Weight
Solid precursors	Granite	729.5 g
	Ground granulated blast furnance slag (GGBFS)	
	Silica flour Microsilica	
Liquid activators	KOH	280.6 g
	Water	46.8 g
Retarders	Zinc salts	4 g
	Potassium salts	2.5 g
Rheology modifier	Sodium superplasticizer	3.5 g
Strength enhancer	Sodium enhancing agent	2
Expansive additives	CaO	0 or 8 g

Table 1—Mix design of the geopolymers.

The mix design has been developed and optimized (e.g., rheology, consistency, and setting time) for surface casing applications. It is pumpable for about 4 hours at 25°C.

Linear Expansion (LE) Test. The annular ring test was used to determine the volumetric changes of the geopolymer with and without the addition of the expansive agents as shown in *API RP 10B* (2005).

- The slurry prepared using the high-speed API mixer was transferred into the annular ring cell and placed into a water bath at 25°C, because the slurry was designed for low-temperature applications.
- Two separate readings were taken in the case of expansion (after 24 hours and 7 days). When measuring shrinkage, a spacer block was used, and the measurement was taken at the end of the test period (7 days) after the spacer block was removed.

Compressive Strength Test. The sample preparation for the compressive strength test was done using a method described by Agista et al. (2022) and Kamali et al. (2021) using a cylinderical mold with dimensions of 50-mm diameter and 102-mm height. The test was conducted in accordance with API standards (*API TR 10TR7* 2017). The samples were prepared, poured into the forms, and cured in an autoclave. They were then cured at 25°C and 34.5 bar (500 psi). Three parallels were measured for each sample using an MTS Criterion® Machine. According , the sample should have a slender ratio of between 1 and 2. Also, the samples were removed from the autoclave and the edges were smoothened. They were then placed into the MTS machine and crushed at a loading rate of 10 kN/min.

Shear Bond Strength Test. A circular casing with a diameter of 12.7 cm and a height of 10 cm was attached to a base using an adhesive and left to cure for 24 hours. A slurry prepared using a high-speed mixer was then poured into the casing and cured at 25°C and 34.5 bar (500 psi) in an autoclave for 7 days. The base was removed, and the sample was pushed out of the casing at a rate of 1 mm/min using an electromechanical press machine. The load was applied until movement of the plug in the casing was observed, and the movement was then monitored. The procedure used for measuring the shear bond strength is presented in **Fig. 1.**

(A) 5-inch casing for Curing of the Slurry

(B) Cured Sample Ready for SBS Test

(C) Push-Out Setup

(D) Completely Pushed Out Plug

Fig. 1—Shear bond strength (SBS) test procedure.

Hydraulic Bond Strength (HBS) Test. For the HBS test, 3.2 L of the sample was prepared using the Hobart N50-60 mixer. The slurry was transferred into a circular casing (diameter 12.7 cm and height 40 cm). The sample was cured for 7 days at 25°C and 34.5 bar. After the curing period, the hydraulic bond test cell was connected to a flowmeter, separator, and nitrogen gas tank. The sample was tested at 5-bar intervals for 30 minutes (minimum testing time for negative pressure testing according to NORSOK D-010). The leakages were monitored via bubbling in the separator and by flowmeter data logging. After the test, the cell was opened and inspected for leaks in the plug. The HBS test is illustrated in **Fig. 2.**

(A) Nitrogen Gas Supply

(B) Hydraulic Sealability Test Cell

(C) Separator

(D) Flow Meters Connected to a Data Logger

(E) Computer

Fig. 2—HBS test setup.

Results and Discussion

Reactivity of CaO in Water. Generally, CaO reacts with water to form Ca $(OH)_2$ and heat. Thus, reaction processes are exothermic. This could be the reason why the ASTM D4644-16 standard (*ASTM D4644-16* 2016) equates the reactivity of CaO to the time required to reach a temperature value of 60°C in a slaking test. In our test, isocalorimetry usually measured the heat evolution of the hydration of the CaO. To be able to estimate the reactivity, the induction time (time elapsed to see an abrupt increase in the evolved heat) and the maximum heat peak were used as criteria to characterize the CaO and also to get an idea of the hydration rates of the samples.

Fig. 3 shows the heat flow of CaO treated at 900°C, 1200°C, and 1400°C vs. time. The shortest induction time and highest heat flow were measured for HT-900, while HT-1400 showed the longest induction time and lowest heat flow.

As detailed in **Fig. 4,** HT-900 has a shorter time to maximum peak and a higher heat peak than the other samples. Accordingly, HT-900 is much more reactive than the samples treated at higher temperatures (HT-1200 and HT-1400). The difference observed can be attributed to two phenomena as proposed by Commandré et al. (2007). The increase in the undesirable sintering effect on the CaO with increased treatment temperature is shown in **Fig. 5.** This effect tends to block reactive spots on the surfaces of the HT-CaO, thus affecting the reactivity. The second phenomenon is the reduction in the specific surface area because of the undesirable sintering effect as the heat treatment temperature is increased. The high reactivity of HT-900 could be attributed to its high specific surface area (inset in **Fig. 4**), which provides a large surface area available for chemical reaction with water. It could also be that the undesirable sintering effect in the HT-900 is less as compared to the HT-1200 and HT-1400 (refer to **Fig. 5**). This causes it to hydrate rapidly upon encountering water, thereby generating a large amount of heat. Increasing the CaO heat treatment temperature to 1200°C and 1400°C resulted in the formation of stone-like samples (adverse effect of the sintering effect), which had to be milled into smaller particles.

The milling had an obvious impact on the particle size distribution for the HT-1200 and HT-1400. From the particle size distribution **(Fig. 6),** the D(90) was computed to be 60.1 μm, 43.4 μm, and 358 μm for HT-900, HT-1200, and HT-1400, respectively. Even though the D(90) of HT-1200 is lower than that of the HT-900 (as a result of the milling of HT-1200 after heat treatment), the HT-900 still had a short induction period and a higher maximum heat peak than that in HT-1200. The possible explanation for this happening could be the adverse sintering effect covering the reactive spots on the HT-1200, thus reducing its hydration rate as shown in **Fig. 5**. In HT-1400, the

sintering effect could be dominant to such an extent as to slow the hydration rate, and the D(90) indicates that there is a formation of agglomerates due to the high temperatures.

LE of the Rock-Based Geopolymers. The LE/shrinkage of geopolymers without CaO (NG) and with CaO is displayed in **Fig. 7a.** Measurements are made after 24 hours and 7 days. The addition of CaO increases the LE of the geopolymers. However, the reactivity of CaO plays an essential role in the magnitude of the LE. The samples containing CaO with the slowest reaction rates (HT-1400) exhibit a much higher LE than the geopolymers containing CaO with lower reaction rates. The expanded ring of HT-1400 geopolymer is shown

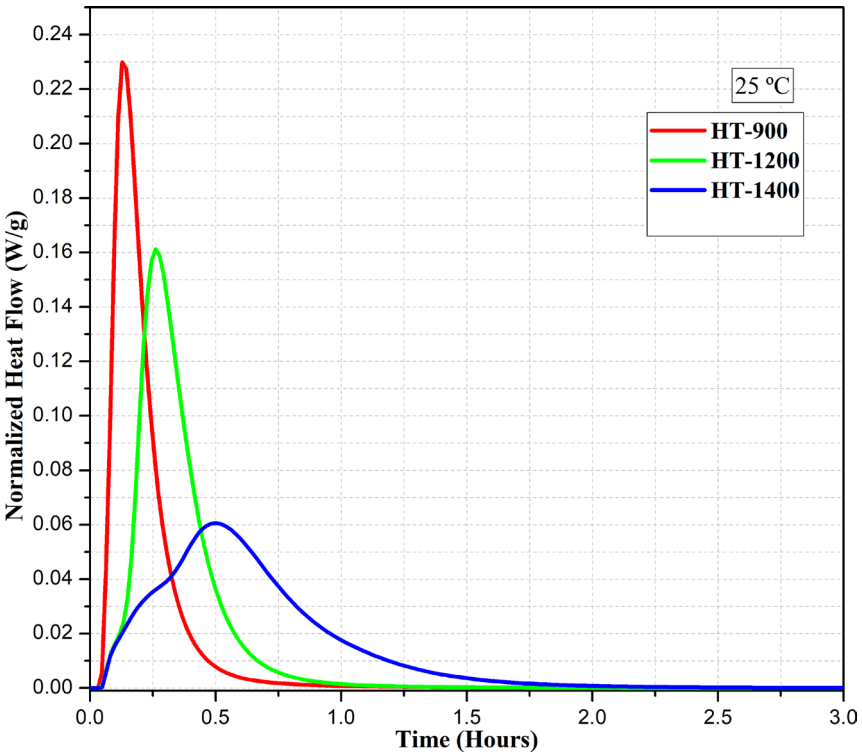

Fig. 3—Heat flow of CaO that has been treated at different temperatures.

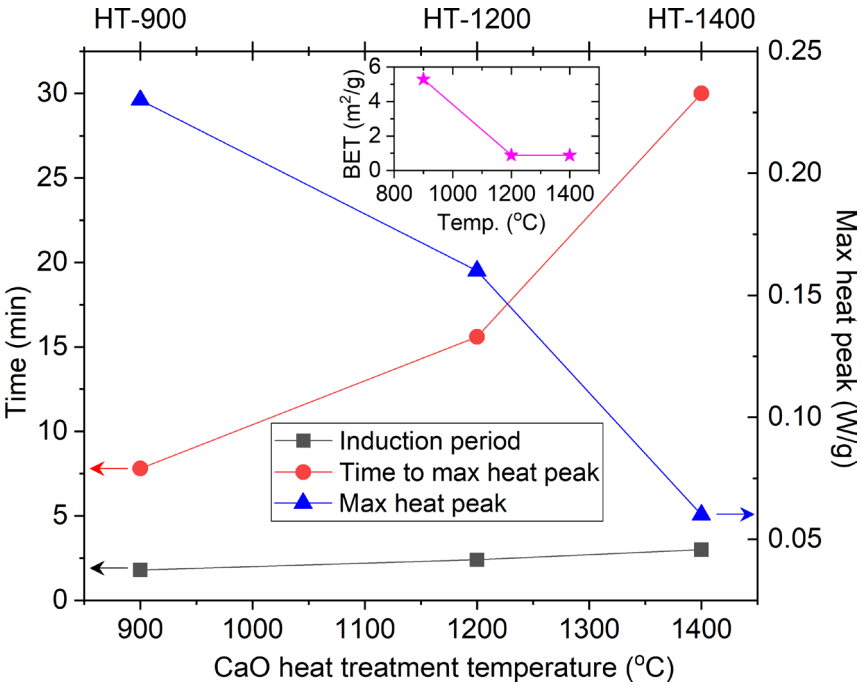

Fig. 4—Induction period, time to maximum peak, and maximum heat peak as a function of the CaO treatment temperature. The inset plot shows the BET specific surface area as a function of the CaO treatment temperature.

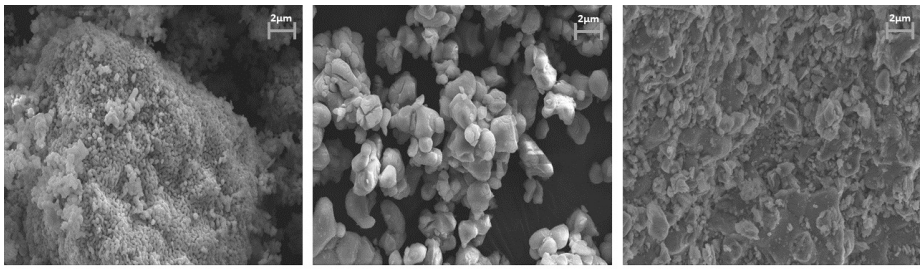

Fig. 5—Effect of heat treatment with increasing temperature.

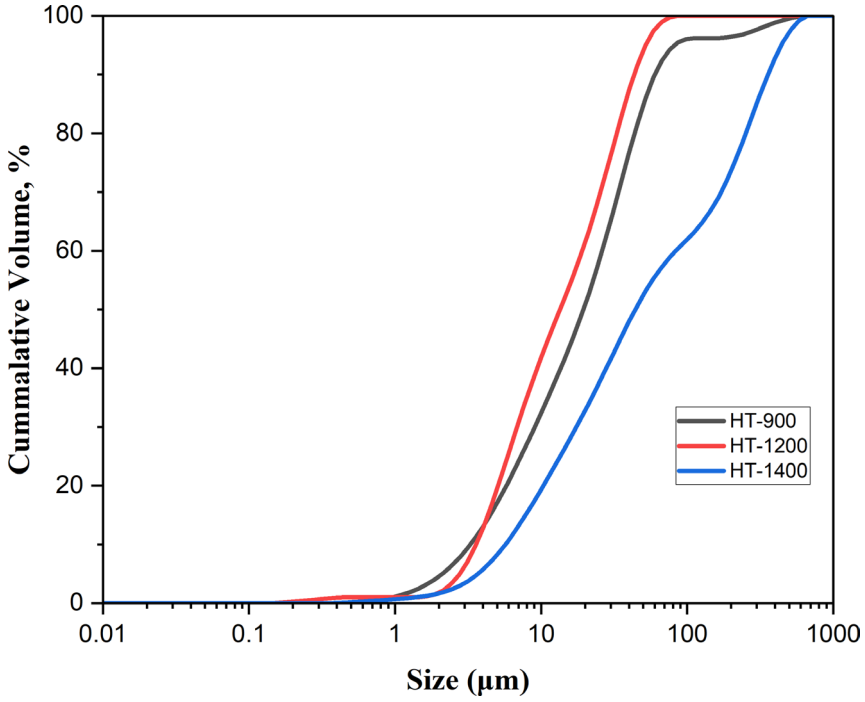

Fig. 6—Particle size distribution of the CaO particles that have been treated at different temperatures.

in **Fig. 7b**. The HT-1400 sample was quite brittle. To examine the correlation between the CaO reaction rate and the LE in more detail, the LE has been plotted as a function of the time to the maximum heat peak (t_{max}) in **Fig. 8.** As can be seen from **Fig. 8**, there is a linear relationship between LE and t_{max} in a log-linear plot, which illustrates an exponential increase. The data have therefore been fitted to:

$$LE = \alpha \cdot \exp(t_{max}/\tau), \quad (1)$$

where α indicates where the fitted line intersects with the y-axis, and τ gives an indication of where the LE increase starts to rise more rapidly (see inset in **Fig. 8**). The fitted values and their errors (one standard deviation) are also displayed in **Fig. 8**. There is no significant difference between the fitted parameters for 1 and 7 days. This indicates that most of the expansion occurs within the first 24 hours. A value of τ close to 600 seconds means that after this time to max heat peak, LE = 2.718α. **Fig. 8** illustrates that samples containing CaO with a t_{max} lower than 10 minutes will have little expansion, while a large expansion occurs when t_{max} is significantly higher than 10 minutes. The enhanced LE at higher t_{max} can be attributed to the presence of supporting structures in the geopolymers at the time of CaO hydration. As can be seen from **Fig. 3**, HT-900 hydrates very quickly; that is, in the early liquid state before the geopolymer has the time to form a supporting structure, the crystal growth can push on to cause expansion. HT-1400 has a significantly slower hydration rate. At this stage, the geopolymer reaction has proceeded long enough for there to be sufficient internal structures to induce the constraint crystal growth pressure to expand the geopolymer. This agrees with studies by Appah and Reichetseder (2001) and Ghofrani and Plack (1993). However, the HT-1400 samples were observed to be very brittle after they were removed from the API ring test cell. In addition, whitish particles (believed to be unreacted CaO) were seen in the matrix (**Fig. 7b**). The brittleness might be caused by crack formation due to excessive internal stresses induced by late hydration of the CaO. Accordingly, the matrix becomes weaker, even though high LE is observed.

Static Shear Bond Strength and Compressive Strength. The shear bond strength and the compressive strength of the geopolymers with and without CaO expansive agents are presented in **Fig. 9.** The bonding of geopolymers to the casing can be grouped into two scenarios, which are the physical effect and the chemical effect. The physical effect comprises the mechanical interlocking and the friction exerted between the geopolymers and casings (Wang et al. 2022). The chemical effect highlights the possibility of the geopolymers reacting with

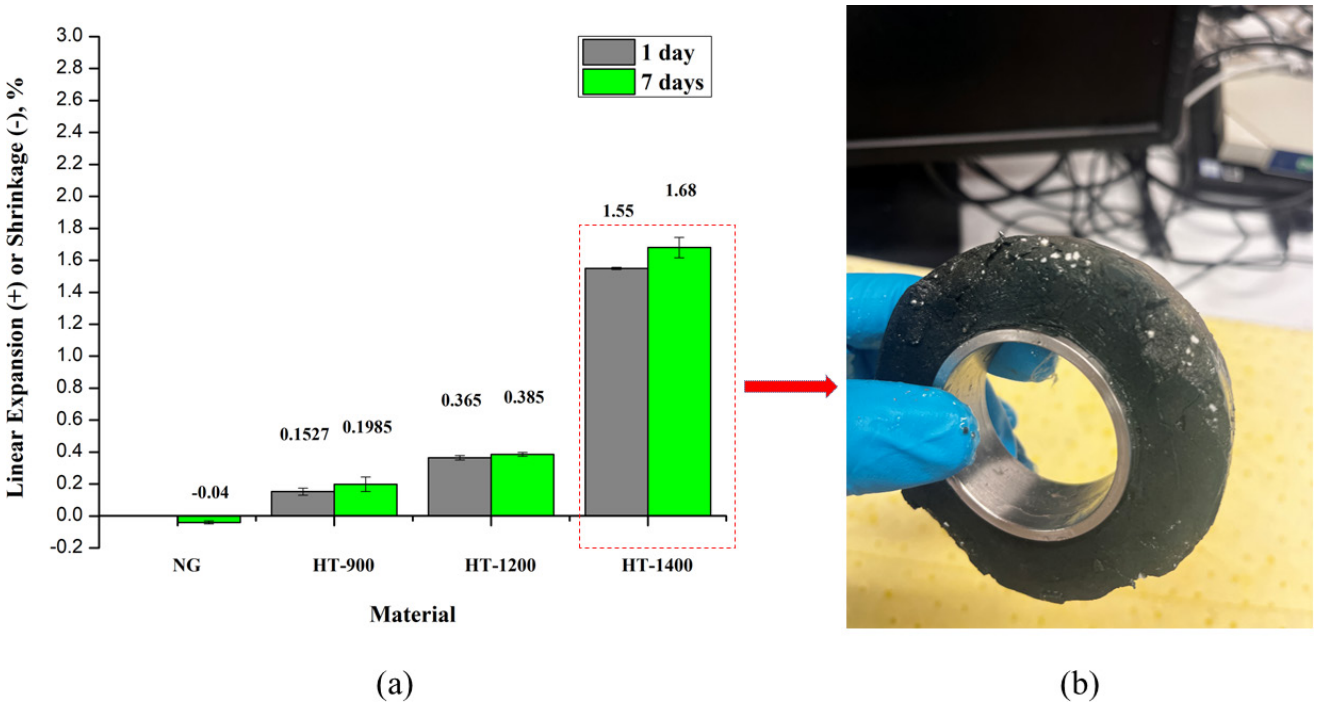

Fig. 7—(a) LE or shrinkage of the different geopolymer mixtures (% circumferential change). (b) Resultant geopolymer in the presence of HT-1400.

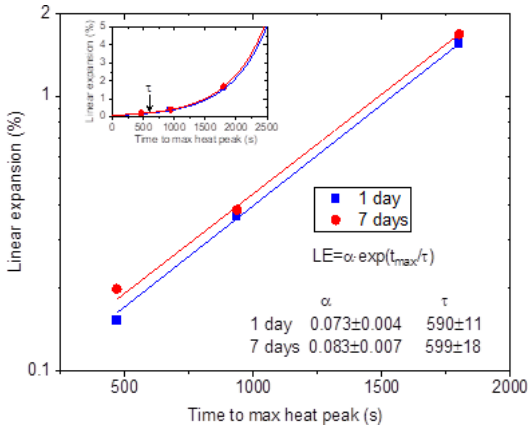

Fig. 8—Relationship between the time to maximum heat peak (t_{max}) and LE after 1 and 7 days with respect to the reactivity of CaO expansive agents. The lines are fitted to Eq. 1, and the fitted parameters are shown in the figure.

the steel to form products at the interface that impact the shear bond strength (Kamali et al. 2022). The introduction of expansive agents to the geopolymer mix increased the shear bond strength. The shear bond strength is enhanced when the CaO reaction rate is slower **(Fig. 4)** and when the LE is raised (**Fig. 7**). The reactivity of the CaO determines the formation of crystals and their growth. The hydrated CaO and its growth could force itself into macropores and cavities at the interfaces, forming large indents at the interface to increase the bond to the casing. This highlights a physical relationship between the measured LE value and the shear bond strength. For the expanding samples, the shear bond strength increases linearly with the LE. The sample without the CaO expansive agent shrinks and therefore exhibits a significantly lower shear bond strength as shown in **Fig. 10.** Even though the shear bond strength increased, the compressive strength of the material decreased with reduced reactivity of the CaO expansive agent. Evans and Carter (1962) highlighted that the compressive strength is directly proportional to the shear bond strength of cement. This contradicts the observed behavior in **Fig. 9**. A possible reason for this discrepancy is the significant expansion of the geopolymers containing CaO with slow reaction rates. The slow hydration rates are coupled with expansion occurring most likely in the hardening phase of the geopolymer, which might cause the destruction of the matrix through excessive crystallization pressure exerted by the hydrating HT-1400 (Ghofrani and Plack 1993), thus giving a lower compressive strength reading. The compressive strength decreases linearly with the LE for the expanding samples (**Fig. 10b**), while the shrinking sample (without CaO) has a smaller compressive strength than the sample with the lowest LE.

Hydraulic Sealability. The HBS test was conducted to estimate the hydraulic sealability at the geopolymer-casting interface **(Fig. 11).** This helps determine the minimum pressure required to start flow at the geopolymer-casing interface. As described by Kamali et al. (2022), the HBS is dependent on the constructive reaction at the barrier material-casing interface, the mechanical indentation that restricts

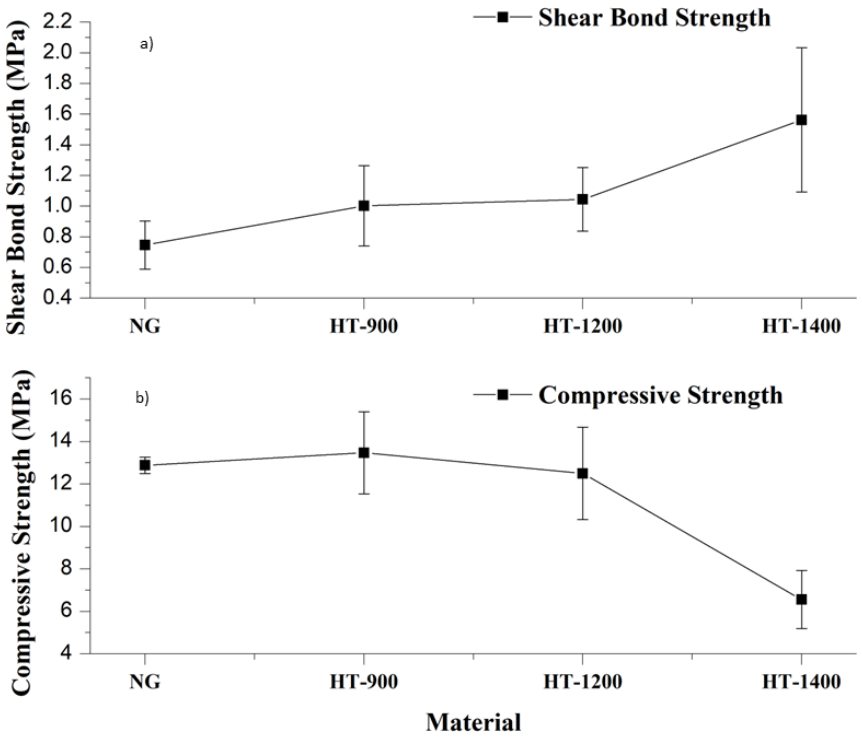

Fig. 9—(a) Shear bond strength and (b) compressive strength of the geopolymer mixes.

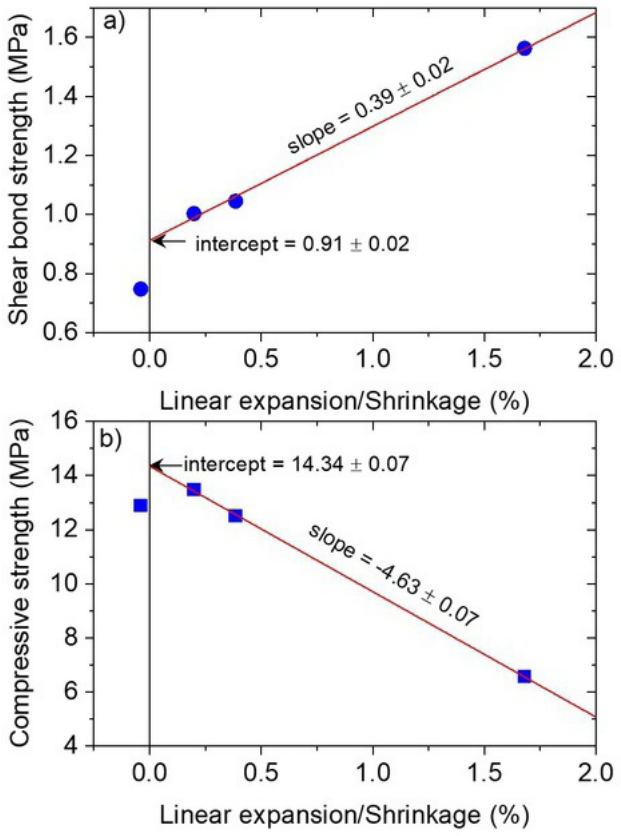

Fig. 10—(a) Shear bond strength and (b) compressive strength as a function of LE/shrinkage after 7 days. The lines are linear fits to the samples that expand.

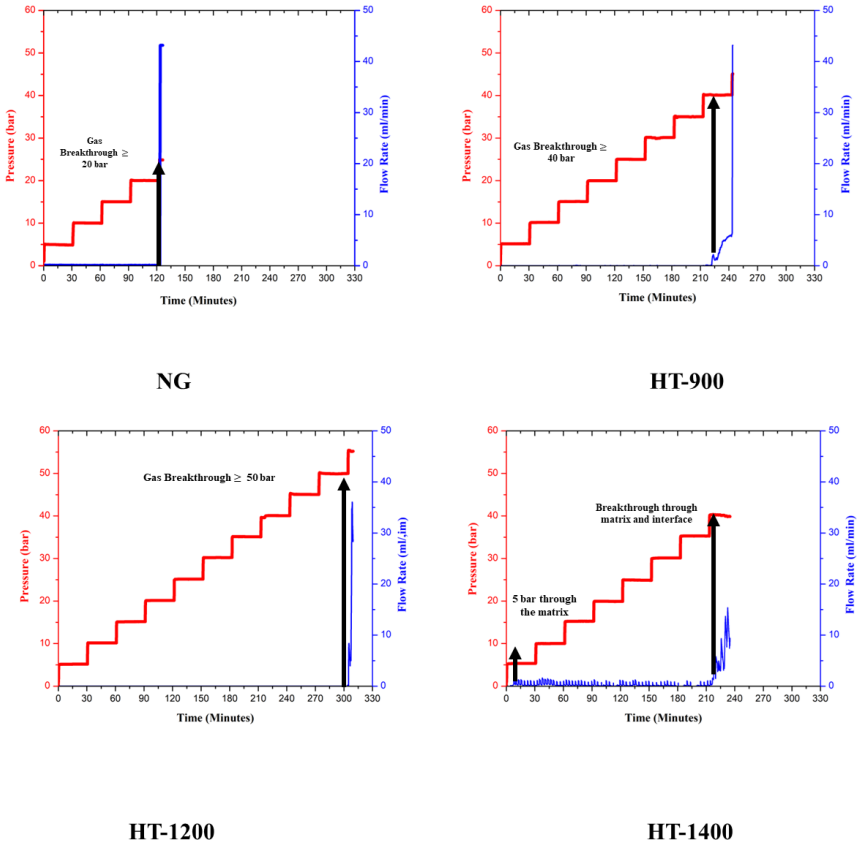

Fig. 11—HBS measurements for the various geopolymers.

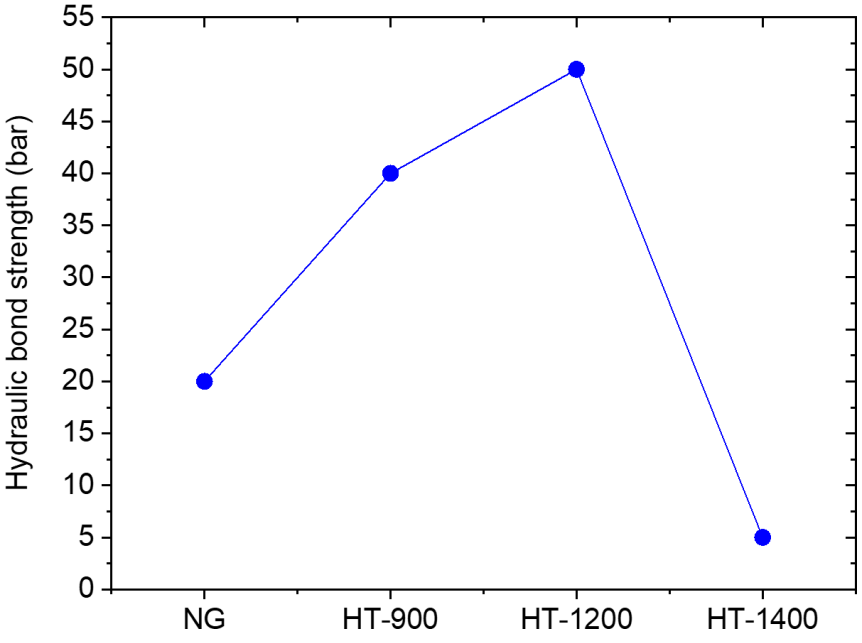

Fig. 12—HBS of the different geopolymers.

flow along the interface, and the permeability of the bulk matrix. The HBS for the different geopolymers is shown in **Fig. 12.** HT-900 and HT-1200 improved the sealability, and leakage was observed to occur at the geopolymer-casing interface. This is due to the existence of the interfacial transition zone, which is deemed to be the weakest link between a cementitious material bonded to a surface. However, in the case of HT-1400, there was leakage through the matrix of the plug, in addition to the leakage at the interface as shown in **Fig. 13.** The leakage through the HT-1400 geopolymer plug agrees with the conjecture of a weaker geopolymer matrix with crack formation due to excessive expansion as discussed in connection with **Fig. 10**. This implies that for the LE to be correlated to the HBS, there should be

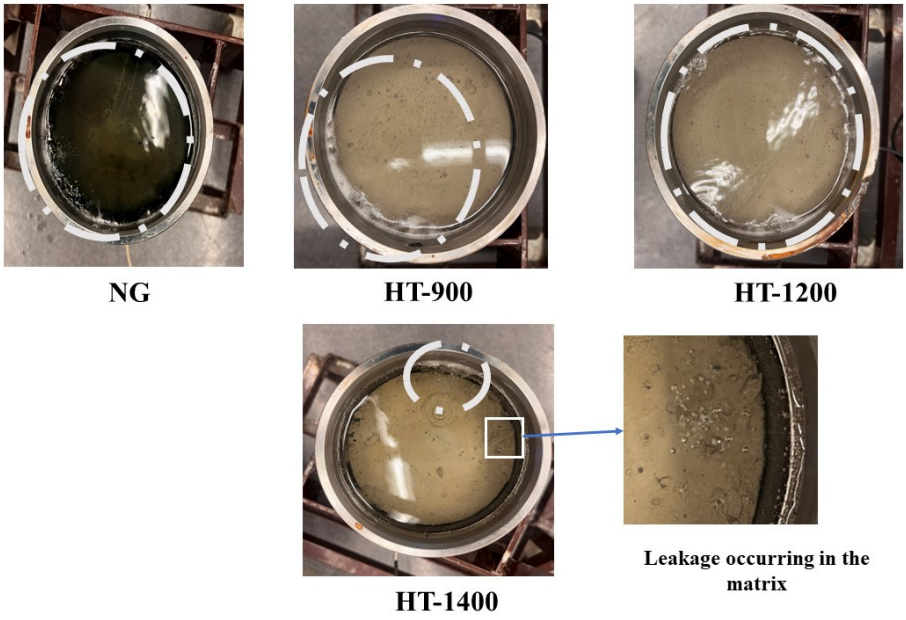

Fig. 13—Leakage pathways in the different geopolymer mixes.

a strong and stabilized matrix in the plug. Accordingly, the HBS increases with the shear bond strength if the matrix is not compromised by excessive crack formation that allows leakage through the geopolymer plug.

Conclusion

The impact of the reactivity of different CaOs, formed by heat treatment at 900°C, 1200°C, and 1400°C, was characterized in terms of their LE, shear bond strength, compressive strength, and HBS. In view of understanding the role of reactivity on the above-stated solid-state properties, it can be concluded that:

- The reactivity of CaO can be controlled using heat treatment of the surfaces. The sintering effect of the surfaces of the CaO reduces the hydration rate.
- Controlling the reactivity of the CaO has impacts on the LE, shear bond strength, and HBS.
- The LE of the geopolymer mixtures increases with decreasing reactivity of the CaO; in other words, slower hydration rates tend to give a higher LE value.
- The shear bond strength increases linearly with the LE. Accordingly, geopolymers containing CaO with slower reaction rates exhibit a larger LE. The underlying mechanism can be a combination of both physical and chemical interactions occurring at the interfaces.
- The compressive strength is linearly reduced with the LE. The compressive strength of the geopolymers will therefore decrease for samples containing CaO with slower reaction rates because of the overexpansion exerted by the slowly hydrating CaO.
- The HBS of the geopolymers can be improved by use of expansive agents, provided there is a stable and strong matrix without cracks after expansion. This can be achieved using an expansive agent that causes moderate expansion without excessive crack formation.

Geopolymers present an alternative for oil and gas cementing operations. From this study, it is recommended that more research is needed to understand the interface properties between the geopolymers and the steel casing.

Acknowledgment

The authors gratefully acknowledge TotalEnergies, AkerBP, ConocoPhillips, and Research Council of Norway for financially supporting the SafeRock KPN Project (RCN 319014 - New Cementitious Material for Oil Well Cementing Applications - SafeRock) at the University of Stavanger, Norway. Special acknowledgement to the Advanced Materials Research Group of Østfold University College.

References

Adjei, S., Elkatatny, S., Aggrey, W. N. et al. 2022. Geopolymer as the Future Oil-Well Cement: A Review. *J Pet Sci Eng* **208** (PB): 109485. https://doi.org/10.1016/j.petrol.2021.109485.

Agista, M. N., Khalifeh, M., and Saasen, A. 2022. Evaluation of Zonal Isolation Material for Low Temperature Shallow Gas Zone Application. Paper presented at the SPE Asia Pacific Oil & Gas Conference and Exhibition, Adelaide, Australia, 17–19 October. SPE-210751-MS. https://doi.org/10.2118/210751-MS.

API RP 10B, *Recommended Practice on Determination of Shrinkage and Expansion of Well Cement Formulations at Atmospheric Pressure*. 2005. Washington, DC, USA: American Petroleum Institute (API).

API RP 10B-2. 2019. *Recommended Practice for Testing Well Cements-Reaffirmed*. Washington, DC, USA: API.

API TR 10TR7. 2017. *Mechanical Behavior of Cement*. Washington, DC, USA: American Petroleum Institute (API).

Appah, D. and Reichetseder, P. 2001. Selection and Use of CaO-Expanding Cements. *Energy Explor Exploit* **19** (6): 581–591. https://doi.org/10.1260/0144598011492697.

Aslani, F., Zhang, Y., Manning, D. et al. 2022. Additive and Alternative Materials to Cement for Well Plugging and Abandonment: A State-of-the-Art Review. *J Pet Sci Eng* **215** (PB): 110728. https://doi.org/10.1016/j.petrol.2022.110728.

ASTM D4644-16, *Standard Test Method for Slake Durability of Shales and Other Similar Weak Rocks*. 2016. West Conshohocken, Pennsylvania, USA: ASTM International.

Chamssine, F., Khalifeh, M., Eid, E. et al. 2021. Effects of Temperature and Chemical Admixtures on the Properties of Rock-Based Geopolymers Designed for Zonal Isolation and Well Abandonment. Paper presented at the ASME 2021 40th International Conference on Ocean, Offshore and Arctic Engineering, Virtual, Online, 21–30 June. OMAE2021-60808. https://doi.org/10.1115/OMAE2021-60808.

Chen, X., Kim, E., Suraneni, P. et al. 2020. Quantitative Correlation between the Degree of Reaction and Compressive Strength of Metakaolin-Based Geopolymers. *Materials* **13** (24): 1–13. https://doi.org/10.3390/ma13245784.

Commandré, J.-M., Salvador, S., and Nzihou, A. 2007. Reactivity of Laboratory and Industrial Limes. *Chem Eng Res Des* **85** (4): 473–480. https://doi.org/10.1205/cherd06200.

Davidovits, J. 1994. Properties of Geopolymer Cements. Paper presented at the First International Conference on Alkaline Cements and Concretes, Kiev, Ukraine, 11–14 October.

Davidovits, J. 2002. Environmentally Driven Geopolymer Cement Applications. Paper presented at the Geopolymer, Melbourne, Australia, 28–29 October.

Davidovits, J. 2013. Geopolymer Cement: A Review. *Geopolymer Science and Technics*. Technical Paper #21.

Davies, R. J., Almond, S., Ward, R. S. et al. 2014. Oil and Gas Wells and Their Integrity: Implications for Shale and Unconventional Resource Exploitation. *Mar Pet Geol* **56**: 239–254. https://doi.org/10.1016/j.marpetgeo.2014.03.001.

Evans, G. W. and Carter, L. G. 1962. Bounding Studies of Cementing Compositions to Pipe and Formations. In *Drilling and Production Practice*. Washington, DC, USA: American Petroleum Institute (API).

Ghofrani, R. and Plack, H. 1993. CaO- and/or MgO-Swelling Cements: A Key for Providing A Better Annular Sealing? Paper presented at the SPE/IADC Drilling Conference, Amsterdam, The Netherlands, 22–25 February. SPE-25697-MS. https://doi.org/10.2523/25697-MS.

Gomado, F. D., Khalifeh, M., and Aasen, J. A. 2023. Expandable Geopolymers for Improved Zonal Isolation and Plugging. Paper presented at the SPE/IADC International Drilling Conference and Exhibition, Stavanger, Norway, 7–9 March. SPE-212493-MS. https://doi.org/10.2118/212493-MS.

Gomado, F. D., Khalifeh, M., Kamali, M. et al. 2022. Sealing Performance of Geopolymer for Plugging and Abandonment; Apple-to-Apple Scenario. Paper presented at the SPE Norway Subsurface Conference, Bergen, Norway, 27 April. SPE-209552-MS. https://doi.org/10.2118/209552-MS.

Humairah, S., Irawan, S., Shafiq, N. et al. 2020. Investigating the Expansion Characteristics of Geopolymer Cement Samples in a Water Bath and Compared with the Expansion of ASTM Class-G Cement. *Heliyon* **6** (2). https://doi.org/10.1016/j.heliyon.2020.e03478.

Jafariesfad, N., Geiker, M. R., Gong, Y. et al. 2017. Cement Sheath Modification Using Nanomaterials for Long-Term Zonal Isolation of Oil Wells: Review. *J Pet Sci Eng* **156** (June): 662–672. https://doi.org/10.1016/j.petrol.2017.06.047.

Kamali, M., Khalifeh, M., Saasen, A. et al. 2021. Alternative Setting Materials for Primary Cementing and Zonal Isolation – Laboratory Evaluation of Rheological and Mechanical Properties. *J Pet Sci Eng* **201**: 108455. https://doi.org/10.1016/j.petrol.2021.108455.

Kamali, M., Khalifeh, M., and Saasen, A. 2022. Bonding Mechanism of Zonal Isolation Materials to Clean and Rusted Casing. *SPE J.* **27** (5): 2613–2627. SPE-209812-PA. https://doi.org/10.2118/209812-PA.

Khalifeh, M. 2016. *Materials for Optimized P & A Performance*. Stavanger, Norway: University of Stavanger.

Khalifeh, M., Todorovic, J., Vrålstad, T. et al. 2017. Long-Term Durability of Rock-Based Geopolymers Aged at Downhole Conditions for Oil Well Cementing Operations. *J Sustain Cem Based Mater* **6** (4): 217–230. https://doi.org/10.1080/21650373.2016.1196466.

Khalili, P., Khalifeh, M., and Saasen, A. 2022. The Effect of Fluid Contamination on Rheological Properties of Geopolymer Materials. Paper presented at the ASME 2022 41st International Conference on Ocean, Offshore and Arctic Engineering, Hamburg, Germany, 5–10 June. OMAE2022-78994. https://doi.org/10.1115/OMAE2022-78994.

Kimanzi, R., Wu, Y., Salehi, S. et al. 2020. Experimental Evaluation of Geopolymer, Nano-Modified, and Neat Class H Cement by Using Diametrically Compressive Tests. *J Energy Resour Technol* **142** (9). https://doi.org/10.1115/1.4046702.

Liu, Y., Upchurch, E. R., Ozbayoglu, E. M. et al. 2023. Gas Migration Model for Non-Newtonian Fluids Under Shut-In Well Conditions. Paper presented at the SPE/IADC International Drilling Conference and Exhibition, Stavanger, Norway, 7–9 March. SPE-212466-MS. https://doi.org/10.2118/212466-MS.

McLellan, B. C., Williams, R. P., Lay, J. et al. 2011. Costs and Carbon Emissions for Geopolymer Pastes in Comparison to Ordinary Portland Cement. *J Clean Prod* **19** (9–10): 1080–1090. https://doi.org/10.1016/j.jclepro.2011.02.010.

Mehta, A. and Siddique, R. 2017. Sulfuric Acid Resistance of Fly Ash Based Geopolymer Concrete. *Constr Build Mater* **146**: 136–143. https://doi.org/10.1016/j.conbuildmat.2017.04.077.

Moreira, P., Khalifeh, M., and Govil, A. 2023. Sealing Ability of Barrier Materials for P&A Application: Investigation of Casing-Barrier Interface. Paper presented at the SPE/IADC International Drilling Conference and Exhibition, Stavanger, Norway, 7–9 March. SPE-212562-MS. https://doi.org/10.2118/212562-MS.

Nahm, J. J., Javanmardi, K., Cowan, K. M. et al. 1994. Slag Mix Mud Conversion Cementing Technology: Reduction of Mud Disposal Volumes and Management of Rig-Site Drilling Wastes. *J Pet Sci Eng* **11** (1): 3–12. https://doi.org/10.1016/0920-4105(94)90058-2.

Nelson, E. B. and Guillot, D. 2006. Well Cementing, 2006: 503–547.

NORSOK Standard D-010, *Well Integrity in Drilling and Well Operations*. 2021. Lysaker, Norway: Standards Norway.

Ogienagbon, A. and Khalifeh, M. 2022. Experimental Evaluation of the Effect of Temperature on the Mechanical Properties of Setting Materials for Well Integrity. *SPE J.* **27** (5): 2577–2589. SPE-209794-PA. https://doi.org/10.2118/209794-PA.

Olvera, R., Panchmatia, P., Juenger, M. et al. 2019. Long-Term Oil Well Zonal Isolation Control Using Geopolymers: An Analysis of Shrinkage Behavior. Paper presented at the SPE/IADC International Drilling Conference and Exhibition, The Hague, The Netherlands, 5–7 March. SPE-194092-MS. https://doi.org/10.2118/194092-MS.

Omran, M., Khalifeh, M., and Saasen, A. 2022. Influence of Activators and Admixtures on Rheology of Geopolymer Slurries for Well Cementing Applications. Paper presented at the SPE Asia Pacific Oil & Gas Conference and Exhibition, Adelaide, Australia, 17–19 October. SPE-210698-MS. https://doi.org/10.2118/210698-MS.

Panchmatia, P., Olvera, R., Genedy, M. et al. 2020. Shrinkage Behavior of Portland and Geopolymer Cements at Elevated Temperature and Pressure. *J Pet Sci Eng* **195**: 107884. https://doi.org/10.1016/j.petrol.2020.107884.

Root, R. L. and Calvert, D. G. 1971. The Real Story of Cement Expansion. Paper presented at the SPE Rocky Mountain Regional Meeting, Billings, Montana, 2–4 June. SPE-3346-MS. https://doi.org/10.2118/3346-MS.

Salehi, S., Ezeakacha, C. P., and Khattak, M. J. 2017. Geopolymer Cements: How Can You Plug and Abandon a Well with New Class of Cheap Efficient Sealing Materials. Paper presented at the SPE Oklahoma City Oil and Gas Symposium, Oklahoma City, Oklahoma, USA, 27–31 March. SPE-185106-MS. https://doi.org/10.2118/185106-MS.

Sambucci, M., Sibai, A., and Valente, M. 2021. Recent Advances in Geopolymer Technology. A Potential Eco-Friendly Solution in the Construction Materials Industry: A Review. *J Compos Sci* **5** (4): 109. https://doi.org/10.3390/jcs5040109.

Vignes, B. 2011. *Contribution to Well Integrity and Increased Focus on Well Barriers in a Lifecycle Aspect*. PhD dissertation, University of Stavanger, Stavanger, Norway.

Vola, G., Sarandrea, L., Mazzieri, M. et al. 2019. Reactivity and Overburning Tendency of Quicklime Burnt at High Temperature. *ZKG International* **72** (10): 20–31.

Vrålstad, T., Todorovic, J., Saasen, A. et al. 2016. Long-Term Integrity of Well Cements at Downhole Conditions. Paper presented at the SPE Bergen One Day Seminar, Grieghallen, Bergen, Norway, 20 April. SPE-180058-MS. https://doi.org/10.2118/180058-MS.

Wang, X., Hu, X., Yang, J. et al. 2022. Research Progress on Interfacial Bonding between Magnesium Phosphate Cement and Steel: A Review. *Constr Build Mater* **342**: 127925. https://doi.org/10.1016/j.conbuildmat.2022.127925.

Zhang, B., Zhu, H., Cheng, Y. et al. 2022a. Shrinkage Mechanisms and Shrinkage-Mitigating Strategies of Alkali-Activated Slag Composites: A Critical Review. *Constr Build Mater* **318**: 125993. https://doi.org/10.1016/j.conbuildmat.2021.125993.

Zhang, B., Zhu, H., Feng, P. et al. 2022b. A Review on Shrinkage-Reducing Methods and Mechanisms of Alkali-Activated/Geopolymer Systems: Effects of Chemical Additives. *J Build Eng* **49**: 104056. https://doi.org/10.1016/j.jobe.2022.104056.

Zheng, D., Ozbayoglu, E., Miska, S. Z. et al. 2022. Cement Sheath Fatigue Failure Prediction by ANN-Based Model. Paper presented at the Offshore Technology Conference, Houston, Texas, USA, 2–5 May. OTC-32046-MS. https://doi.org/10.4043/32046-MS.